Title

Multiple Mechanisms for E2F Binding Inhibition by Phosphorylation of the Retinoblastoma Protein C-Terminal Domain

Journal

Journal of Molecular Biology, 426(1)

ISSN

0022-2836

Authors

Burke, Jason R
Liban, Tyler J
Restrepo, Tamara
et al.

Publication Date

2014

DOI

10.1016/j.jmb.2013.09.031

Peer reviewed

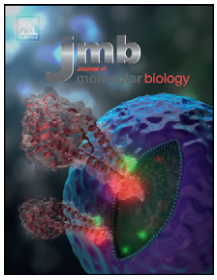

Multiple Mechanisms for E2F Binding Inhibition by Phosphorylation of the Retinoblastoma Protein C-Terminal Domain

Jason R. Burke, Tyler J. Liban, Tamara Restrepo, Hsiau-Wei Lee and Seth M. Rubin

Department of Chemistry and Biochemistry, *University of California Santa Cruz, CA 95064, USA*

Correspondence to Seth M. Rubin: *srubin@ucsc.edu*
http://dx.doi.org/10.1016/j.jmb.2013.09.031
Edited by S. Khorasanizadeh

Abstract

The retinoblastoma protein C-terminal domain (RbC) is necessary for the tumor suppressor protein's activities in growth suppression and E2F transcription factor inhibition. Cyclin-dependent kinase phosphorylation of RbC contributes to Rb inactivation and weakens the Rb-E2F inhibitory complex. Here we demonstrate two mechanisms for how RbC phosphorylation inhibits E2F binding. We find that phosphorylation of S788 and S795 weakens the direct association between the N-terminal portion of RbC (RbC^{N}) and the marked-box domains of E2F and its heterodimerization partner DP. Phosphorylation of these sites and S807/S811 also induces an intramolecular association between RbC and the pocket domain, which overlaps with the site of E2F transactivation domain binding. A reduction in E2F binding affinity occurs with S788/S795 phosphorylation that is additive with the effects of phosphorylation at other sites, and we propose a structural mechanism that explains this additivity. We find that different Rb phosphorylation events have distinct effects on activating E2F family members, which suggests a novel mechanism for how Rb may differentially regulate E2F activities.

Introduction

The retinoblastoma protein (Rb) is a broad-functioning tumor suppressor that is frequently deregulated in human cancers [1,2]. The loss of functional Rb is associated with several hallmarks of cancer including chromosomal instability and aberrant cell proliferation. Rb acts as a negative regulator of cell division at the G_1–S transition of the cell cycle [3–6]. In G_0 and early G_1, Rb forms a growth-repressive complex with E2F transcription factors [7,8]. The Rb-E2F complex is stabilized through two cohesive interactions (Fig. 1a and b): the pocket domain of Rb binds and represses the E2F transactivation domain ($E2F^{TD}$) [9–11], and the C-terminal domain of Rb (RbC) associates with the E2F-DP marked-box and coiled-coil domains ($E2F\text{-}DP^{CM}$) [12–14]. These structured interactions are consistent with the finding that both the pocket domain and RbC are required for full growth suppression and E2F binding [15–17].

Cyclin-dependent kinases (CDKs) phosphorylate Rb at specific CDK-consensus sites in late G_1 (Fig. 1) [3–6,18–21]. Hyperphosphorylated Rb dissociates from E2F, allowing for up-regulation of E2F-mediated transcription and entry into S-phase [15,22,23]. Protein crystal structures have revealed how several key phosphorylation events induce conformational changes to Rb that disrupt the Rb-E2F interfaces (Fig. 1c) [24]. Phosphorylation of S608/S612 in the pocket loop (Rb^{PL}) promotes a binding interaction between Rb^{PL} and the pocket domain that is structurally analogous to the Rb-$E2F^{TD}$ binding interaction [25,26]. Phosphorylation of T373 in the interdomain linker (Rb^{IDL}) stabilizes binding between the pocket domain and the N-terminal domain (RbN), inducing an allosteric change to the $E2F^{TD}$ binding site in the pocket [26,27]. Phosphorylation of T821 and T826 in RbC also induces an intramolecular association between RbC and the pocket at the "LxCxE" binding site [14,28,29]; data suggest that this interaction dissociates proteins involved in chromatin remodeling and gene silencing [28]. Quantitative binding studies have revealed that phosphorylation of sites in RbC also reduces binding between RbC and $E2F1\text{-}DP1^{CM}$, although this inhibitory mechanism has not been clarified [14].

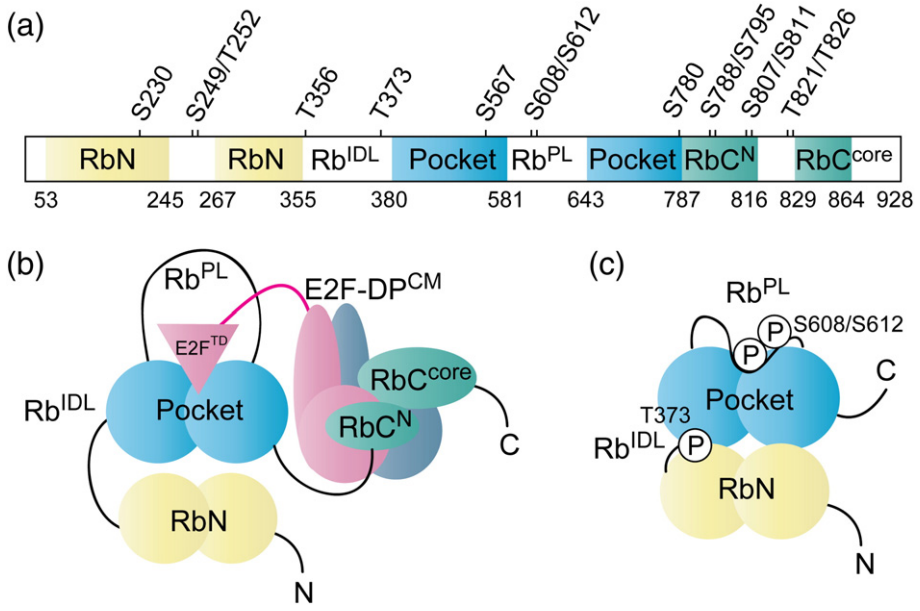

Fig. 1. Schematic of Rb protein structure. (a) Domain organization and CDK-consensus phosphorylation sites. Structured domains are colored, unstructured domains are uncolored, and domain boundaries used in this study are indicated. (b) Summary of interactions that contribute to the overall Rb-E2F complex. The Rb pocket domain binds the E2F transactivation domain ($E2F^{TD}$), while the Rb C-terminal domain (RbC) binds the E2F-DP coiled-coil and marked-box ($E2F\text{-}DP^{CM}$) domains. (c) Summary of previously characterized phosphorylation events and their structural effects that disrupt the Rb-$E2F^{TD}$ complex. Phosphorylation of S608/S612 in the pocket loop (Rb^{PL}) induces binding of Rb^{PL} to the pocket at the $E2F^{TD}$ site. Phosphorylation of T373 in the interdomain linker (Rb^{IDL}) induces N-terminal domain (RbN) docking to the pocket, which allosterically disrupts the $E2F^{TD}$-binding cleft.

RbC phosphorylation is a critical component of E2F activation and is necessary for full transactivation activity at E2F-bound promoters [30,31]. Here we therefore sought to determine whether RbC phosphorylation destabilizes binding between Rb and the E2F transactivation domain. In this study, we use isothermal titration calorimetry (ITC) and nuclear magnetic resonance (NMR) to observe phosphorylation-dependent changes in binding between Rb and E2F. We find that phosphorylation of S788 and S795 in the N-terminal region of RbC (RbC^N) inhibits the Rb-$E2F^{TD}$ association by inducing binding of RbC^N to the pocket domain. In addition, phosphorylation of RbC^N abrogates the association between RbC^N and the $E2F1\text{-}DP1^{CM}$ complex. We find that phosphorylation of RbC^N at S788/S795 is additive to the effects of Rb^{IDL} and Rb^{PL} phosphorylation in inhibiting Rb-$E2F^{TD}$ binding, indicating that structural compatibilities exist between these distinct mechanisms. Finally, we identify differences in how these phosphorylation-induced inhibitory mechanisms affect the binding of paralogous "activating" $E2F^{TD}$s (E2F1–3) to Rb. Together, these binding studies contribute to a complete understanding of how specific post-translational phosphorylation events regulate the distinct functional interfaces of this critical cell cycle regulatory protein.

Results

RbC^N (S788/S795) phosphorylation inhibits $E2F1^{TD}$ binding to Rb pocket by ITC

We used ITC to measure binding affinities of $E2F1^{TD}$ (residues 372–437) for a series of Rb constructs, each engineered to contain specific RbC^N phosphorylation sites (Table 1 and Supplementary Fig. S1). The proteins were phosphorylated quantitatively with recombinant CDK as needed (Supplementary Fig. S2). We first tested binding of $E2F1^{TD}$ to an Rb construct ($Rb^{380\text{-}816\Delta PL/S780A}$) that contains the pocket domain and four phosphoacceptor sites (S788/S795/S807/S811) but lacks the Rb^{PL} sites (S608/S612) and S780. S780 phosphorylation does not influence $E2F^{TD}$ binding [25], and the S780A mutation facilitates homogeneous phosphorylation in the preparative *in vitro* kinase reaction. We found that $E2F1^{TD}$ binds to phosphorylated $Rb^{380\text{-}816\Delta P/S780A}$ (K_d = 0.47 ± 0.04 μM) with an affinity that is 7-fold weaker than its affinity for unphosphorylated protein (K_d = 0.07 ± 0.03 μM). When both S807 and S811 are substituted for alanine in this construct, $E2F1^{TD}$ retains the reduced binding affinity for phosphorylated Rb (K_d = 0.51 ± 0.07 μM). This result indicates that

Table 1. ITC measurements of the effect of RbC^N phosphorylation on $E2F1^{TD}$ binding

Rb construct	Available CDK sites	UnphosRb-$E2F1^{TD}$ K_d (μM)	PhosRb-$E2F1^{TD}$ K_d (μM)
$380\text{-}816^{\Delta PL/S780A}$	S788/S795/S807/S811	0.07 ± 0.03	0.47 ± 0.04
$380\text{-}816^{\Delta PL/S780A/S807A/S811A}$	S788/S795	0.08 ± 0.02	0.51 ± 0.07
$380\text{-}816^{\Delta PL/S780A/S788A/S795A}$	S807/S811	0.09 ± 0.03	0.13 ± 0.06
$380\text{-}800^{\Delta PL/S780A}$	S788/S795	0.05 ± 0.01	0.5 ± 0.1
$380\text{-}794^{\Delta PL/S780A}$	S788	0.12 ± 0.01	0.27 ± 0.02

ITC data are shown in Supplementary Fig. S1.

S807 and S811 do not contribute to the inhibition of the Rb-$E2F1^{TD}$ interaction.

When both S788 and S795 are substituted to alanine, we find that phosphorylated Rb (K_d = 0.13 ± 0.06 μM) binds $E2F1^{TD}$ similar to unphosphorylated Rb (K_d = 0.09 ± 0.03 μM), demonstrating that phosphorylation of S788 and S795 negatively affects Rb-$E2F1^{TD}$ binding. Consistent with this result, we observe reduced $E2F1^{TD}$ binding to a phosphorylated construct that is truncated to exclude both S807 and S811 and contains the S780-to-alanine mutation. This construct ($Rb^{380\text{-}800\Delta PL/S780A}$) has only two intact phosphoacceptor sites (S788 and S795) and binds $E2F1^{TD}$ 10-fold more weakly when it is phosphorylated (K_d = 0.51 ± 0.10 μM) compared to unphosphorylated (K_d = 0.05 ± 0.01 μM). A similar construct, truncated to include only phosphorylation at S788 ($Rb^{380\text{-}794\Delta PL/S780A}$), has a relatively minor effect [K_d = 0.27 ± 0.02 μM (phosphorylated) and K_d =0.12 ± 0.01 μM (unphosphorylated)]. In summary, these results reveal that phosphorylation of RbC^N at S788/S795 negatively regulates binding between $E2F1^{TD}$ and the Rb pocket domain.

Phosphorylation of RbC^N induces binding to Rb pocket

Rb^{PL} phosphorylation on S608/S612 induces an intramolecular association with the pocket domain that overlaps with the $E2F^{TD}$-binding cleft [25,26]. We hypothesized that phosphorylation of RbC^N similarly promotes intramolecular binding to the pocket domain. To test this idea, we generated ^{15}N-labeled RbC^N peptide ($RbC^{787\text{-}816}$) to detect the association *in trans* by NMR. This fragment is phosphorylated on S788, S795, S807, and S811. The $^1H–^{15}N$ heteronuclear single quantum coherence (HSQC) spectrum of the phosphorylated, ^{15}N-labeled $RbC^{787\text{-}816}$ alone shows minimal peak dispersion in the proton dimension, typical of intrinsically disordered polypeptides. Titration of unlabeled Rb pocket into the sample reveals small chemical shift changes and considerable broadening for several peaks (Fig. 2a and b). The broadening is protein concentration dependent (Fig. 2b) and anticipated for binding between the relatively small labeled peptide and the larger unlabeled pocket domain (molecular mass, ~43 kDa). Binding between phosphorylated $RbC^{787\text{-}816}$ and the pocket domain is too weak to be detected *in trans* by ITC (data not shown); this weak binding (K_d > ~100 μM) is consistent with the high protein concentrations needed to observe the broadening effect in the NMR experiment. Peak broadening is not observed for the ^{15}N-labeled unphosphorylated peptide in the presence of excess Rb pocket, demonstrating that the RbC^N-Rb pocket interaction is dependent on phosphorylation of the RbC^N peptide (Fig. 2c and Supplementary Fig. S3).

NMR peaks in the phosphorylated $RbC^{787\text{-}816}$ spectrum were assigned using standard methods. The peaks that undergo the most pronounced broadening correspond to clusters of residues surrounding phosphorylated S788, S795, and S807 (Fig. 2b). The most straightforward interpretation of this result is that residues in these sequences directly contact the pocket domain. However, we cannot rule out the possibility that a subset of these spectral perturbations result from structural changes in RbC^N that occur upon association. Peaks corresponding to residues surrounding S807 are influenced in the pocket titration, even though these residues do not contribute to inhibition of $E2F1^{TD}$ in the ITC assay. The chemical environments of these residues are perhaps influenced by pocket binding in a manner that is independent of the effect of phosphorylated RbC on E2F inhibition. We next tested whether binding of phosphorylated RbC^N and $E2F^{TD}$ to the pocket is mutually exclusive. We titrated a labeled, phosphorylated RbC^N sample with unlabeled Rb pocket that is first saturated with 1 molar equivalent of $E2F2^{TD}$. In this case, we observe reduced peak broadening effects, demonstrating that $E2F^{TD}$ competes with phosphorylated RbC^N in binding the pocket (Fig. 2b and d).

We examined the structure of the pocket-$E2F2^{TD}$ complex to identify potential binding sites between the pocket and phosphorylated RbC^N (Fig. 3a). We found two clusters of conserved side chains that are capable of coordinating a phosphate. These side chains make interactions with $E2F^{TD}$ that would likely be disrupted by RbC^N binding and are in close proximity to the structured C-terminus of the pocket (I785 in the $E2F2^{TD}$-pocket structure) [10]. One site is near K652

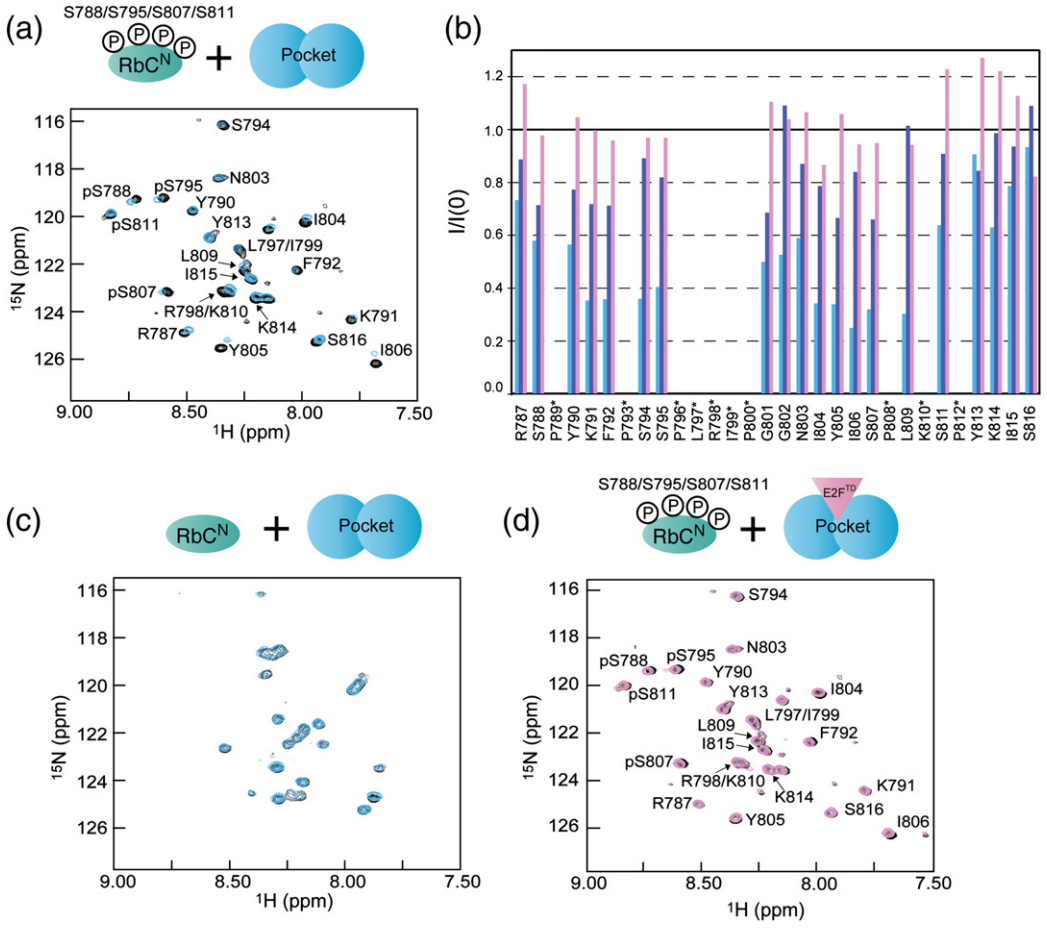

Fig. 2. Phosphorylation of RbC$^{787\text{-}816}$ promotes intramolecular binding to the Rb pocket domain. (a) ^{1}H–^{15}N HSQC spectra of 50 μM ^{15}N-labeled phosphorylated RbC$^{787\text{-}816}$ alone (black) and in the presence of 900 μM unlabeled Rb pocket$^{380\text{-}787\Delta PL}$ (cyan). Broadening of select resonance peaks indicates an *in trans* association between the phosphorylated RbC^{N} peptide and the pocket domain. (b) The ratio of peak intensity in the presence (*I*) and in the absence [*I*(0)] of pocket domain is plotted for each residue in phosRbC$^{787\text{-}816}$. Ratios are plotted for addition of 300 μM (dark blue) and 900 μM (cyan) unlabeled Rb pocket$^{380\text{-}787\Delta PL}$ and for addition of 900 μM pocket in the presence of 900 μM unlabeled E2F2^{TD} (red). Intensity ratios were not quantified for overlapping peaks and prolines, marked with an asterisk (*). (c) HSQC spectra of 60 μM ^{15}N-labeled unphosphorylated RbC$^{787\text{-}816}$ alone (black) and in the presence of 900 μM unlabeled Rb pocket$^{380\text{-}787\Delta PL}$ (cyan). The absence of peak broadening indicates a lack of binding between unphosphorylated RbC$^{787\text{-}816}$ and Rb pocket, which demonstrates that binding between RbC$^{787\text{-}816}$ and the pocket is dependent upon phosphorylation. The ratio of peak intensities in the presence and absence of pocket domain are plotted in Supplementary Fig. S3. (d) ^{1}H–^{15}N HSQC spectra of 50 μM ^{15}N-labeled phosphorylated RbC$^{787\text{-}816}$ alone (black) and in the presence of 900 μM unlabeled Rb pocket$^{380\text{-}787\Delta PL}$ and 900 μM unlabeled E2F2^{TD} (pink). The signal-broadening, plotted in (b), is less extensive than in the absence of E2F2^{TD}, suggesting that binding between E2F2^{TD} and Rb pocket excludes phosphorylated RbC$^{787\text{-}816}$.

and R656. K652 forms a salt bridge with E417 in E2F2. A second potential site is formed by K548, H555, R661, and H733. K548 and H555 hydrogen bond with D410 and D411 in E2F2^{TD}, respectively. We used the NMR assay to examine whether mutation of these sites influences the binding of phosRbC^{N} to the pocket domain (Fig. 3b). We added unlabeled wild type, K652A/R656A, and H555A/H733A pocket to ^{15}N-labeled phosRbC$^{787\text{-}816}$ and compared the line-broadening in the spectra. The K652A/R656A pocket mutant shows reduced broadening consistent with loss of affinity, while the H555A/H733A mutant shows similar behavior as wild type. These data indicate that phosRbC^{N} binding requires an interaction with the conserved K652/R656 site in the pocket.

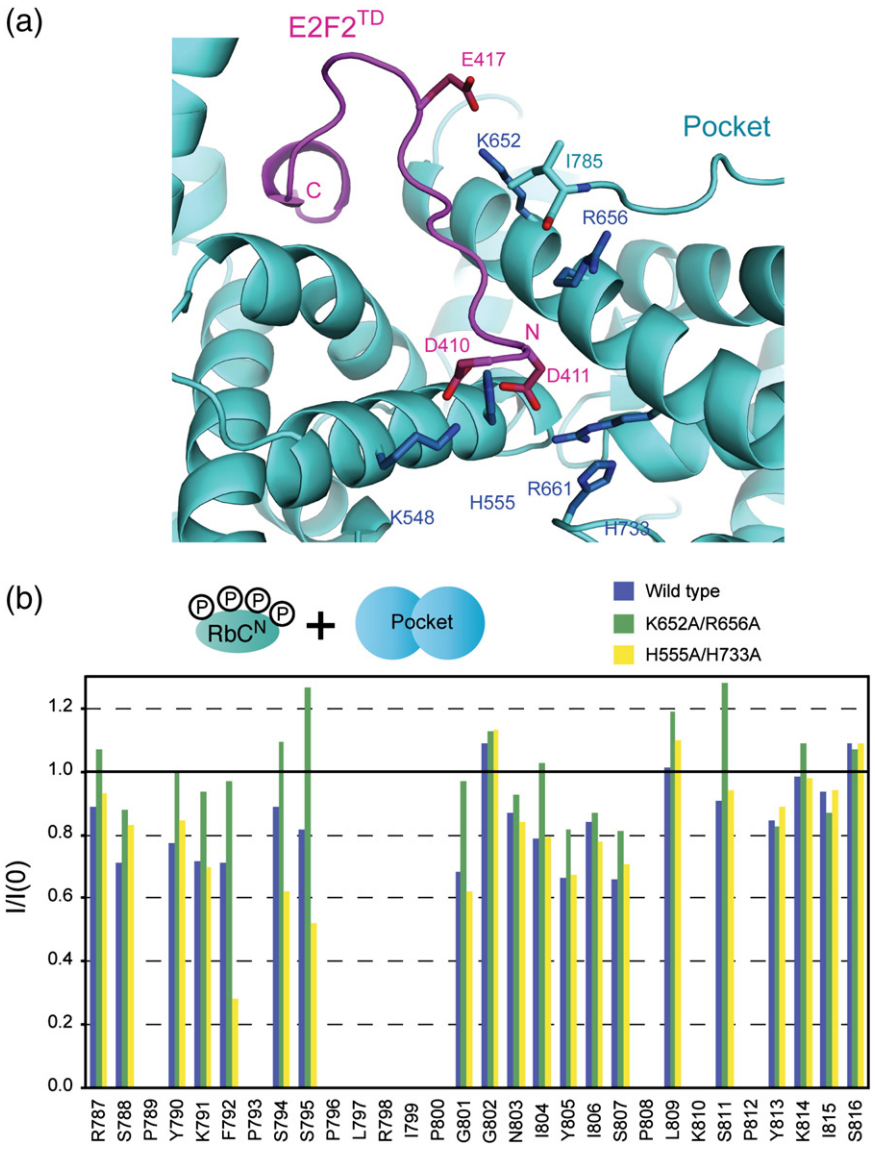

Fig. 3. Phosphorylated RbC^{N} binds the pocket domain at a site that overlaps the E2F^{TD} binding site. (a) Putative interactions sites in the pocket domain for phosphorylated RbC^{N} side chains. The structure of the E2F2^{TD}-pocket complex is shown (PDB code: 1N4M) along with two clusters of residues that could be reached by S795 (K548, H555, R661, and H733) and S788 or S795 (K652 or R656). Binding of RbC^{N} in this region of the pocket would disrupt interactions with the N-terminal portion of E2F^{TD}. (b) Mutation of K652/R656 but not H555/H733 inhibits binding of phosRbC^{N} to the pocket domain. The ratio of peak intensity in the presence (I) and in the absence [I(0)] of 300 μM wild type (dark blue), K652A/R656A (green), and H555A/H733A (yellow) pocket domain is plotted for each residue in phosRbC$^{787\text{-}816}$. The K652A/R656A mutant induces relatively less line-broadening, suggesting that the association depends on those residues.

Phosphorylation of RbC^{N} dissociates RbC^{N} from E2F1-DP1^{CM}

It has been observed that that phosphorylation of S788/S795 in the context of the entire RbC (residues 771–928) weakens the RbC affinity for E2F1-DP1^{CM} [14]. However, because RbC^{N} was not included in the ternary complex that crystallized, the mechanism has not been characterized. We examined here whether RbC^{N} binds directly with E2F1-DP1^{CM} and whether this association is modulated by S788/S795 phosphorylation. We collected ^{1}H–^{15}N HSQC spectra of unphosphorylated ^{15}N-labeled RbC$^{787\text{-}816}$ both alone and in the presence of unlabeled E2F1-DP1^{CM} (Fig. 4a). By comparing the spectra, we observe extensive signal-broadening indicative of complex formation between unphosphorylated RbC^{N} and E2F1-DP1^{CM}. When we conduct this experiment using phosphorylated ^{15}N-labeled RbC^{N}, we see less signal-broadening (Fig. 4b), suggesting that

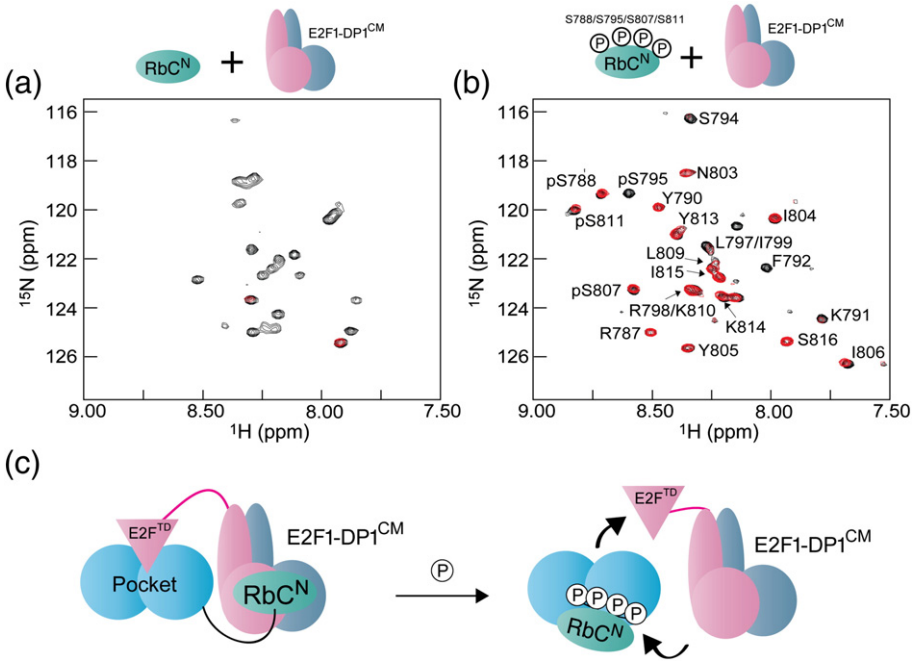

Fig. 4. Phosphorylation of RbC$^{787\text{-}816}$ abrogates binding between RbC^{N} and E2F1-DP1^{CM}. (a) ^{1}H–^{15}N HSQC spectra of 60 μM ^{15}N-labeled unphosphorylated RbC$^{787\text{-}816}$ alone (black) and in the presence of 300 μM unlabeled E2F1-DP1^{CM} (red). The peak broadening observed in this spectrum indicates binding. (b) HSQC spectra of 100 μM ^{15}N-labeled phosphorylated RbC$^{787\text{-}816}$ alone (black) and in the presence of 300 μM unlabeled E2F1-DP1^{CM} (red). Less peak broadening is observed here than in (a), indicating that phosphorylation of RbC$^{787\text{-}816}$ inhibits the RbC-E2F1-DP1^{CM} complex. (c) Summary of interactions identified by NMR: phosphorylated RbC$^{787\text{-}816}$ dissociates from E2F1-DP1^{CM} and associates with Rb pocket in a manner that is inconsistent with E2F^{TD} binding.

phosphorylation of RbC^{N} destabilizes the direct binding interaction with E2F-DP1^{CM}. Taken together with the NMR data demonstrating an RbC^{N}-pocket interaction (Fig. 2), these results suggest that RbC^{N} phosphorylation has two distinct roles in disrupting the overall Rb-E2F complex (Fig. 4c). First, phosphorylation of RbC^{N} destabilizes the direct association between RbC^{N} and E2F1-DP1^{CM}. Second, phosRbC^{N} binds the pocket domain to destabilize the E2F1^{TD} interaction.

Phosphorylation of RbC^{N} is additive with the effects of Rb^{PL} and Rb^{IDL} phosphorylation in inhibiting E2F1^{TD}-Rb pocket binding

With these observed effects of RbC^{N} phosphorylation, we have now identified three distinct structural mechanisms by which Rb phosphorylation inhibits E2F1^{TD} binding to the pocket domain. Phosphorylation of Rb^{IDL} (T356/T373) induces RbN-pocket docking and inhibits Rb-E2F1^{TD} binding approximately 45-fold [25,26]. Most of this effect is attributable to T373 phosphorylation alone, which mediates the conformational change, although T356 phosphorylation does enhance the inhibition of Rb-E2F1^{TD} binding [26]. Phosphorylation of Rb^{PL} at S608 induces association of Rb^{PL} and the pocket, which inhibits Rb-E2F1^{TD} binding approximately 10-fold. S612 phosphorylation alone in Rb^{PL} reduces E2F1^{TD} binding 3-fold but has no additive effect when S608 is also phosphorylated [25,26]. Finally, we report here that phosphorylation of S788 and S795 in RbC^{N} induces an association with the pocket domain, which inhibits Rb-E2F1^{TD} binding approximately 7-fold.

We previously found that Rb^{PL} and Rb^{IDL} phosphorylation together have an additive effect in inhibiting Rb-E2F1^{TD} [25]. We next investigated whether RbC^{N} phosphorylation contributes additively to the inhibitory effects of Rb^{PL} and Rb^{IDL} phosphorylation. We first generated an Rb construct (Rb$^{380\text{-}816}$) that contains both the RbC^{N} (S788/S795) and Rb^{PL} (S608/S612) phosphorylation sites but lacks RbN and the Rb^{IDL} (T356/T373) phosphorylation sites. E2F1^{TD} binds unphosphorylated Rb$^{380\text{-}816/780A}$ with a K_d of 0.07 ± 0.03 μM and phosphorylated Rb$^{380\text{-}816/780A}$ with a K_d of 3.1 ± 0.5 μM (Fig. 5a and b). This 45-fold reduction in E2F1^{TD} binding is nearly the product of the 10-fold and 7-fold effects observed independently, indicating that the Rb^{PL} and RbC^{N} mechanisms work together to inhibit the Rb-E2F1^{TD} complex.

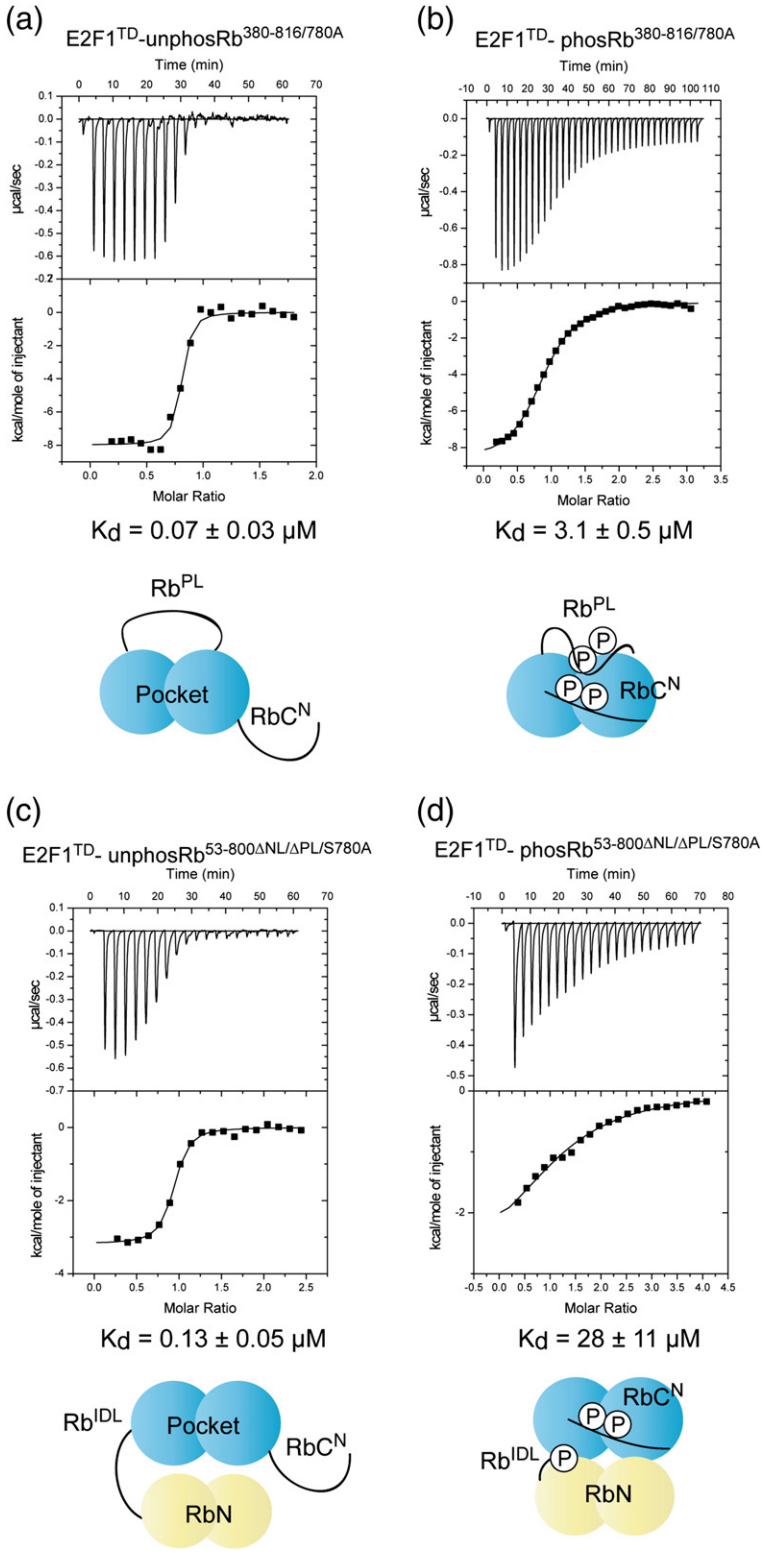

Fig. 5. ITC data demonstrate that Rb-E2F binding inhibition occurs through the additive effects of multiple mechanisms. Dissociation constants were determined from binding isotherms of $E2F1^{TD}$ with (a) unphosphorylated $Rb^{380\text{-}816/780A}$, (b) phosphorylated $Rb^{380\text{-}816/780A}$, (c) unphosphorylated $Rb^{53\text{-}800\Delta NL/\Delta PL/S780A}$, and (d) phosphorylated $Rb^{53\text{-}800\Delta NL/\Delta PL/S780A}$. As shown in the schematic diagrams, these constructs each contain elements needed for two inhibitory mechanisms. Their phosphorylation results in reduced affinity that is greater than constructs containing single inhibitory mechanisms.

To test whether RbC^N and Rb^{IDL} phosphorylation similarly add in inhibiting $E2F^{TD}$ binding, we used a construct of Rb that contains RbN, Rb^{IDL}, the pocket, and RbC^N but lacks the large loops in the pocket and RbN ($Rb^{55\text{-}800\Delta NL/\Delta PL/S780A}$). We observe that $E2F1^{TD}$ binds 230-fold more weakly when this Rb construct is phosphorylated (K_d = 30 ± 10 μM) compared to when it is unphosphorylated (K_d = 0.13 ± 0.05 μM) (Fig. 5c and d). RbC^N and Rb^{IDL} phosphorylation mechanisms are therefore also additive, as phosphorylation at these sites has a 7-fold and 45-fold effect alone, respectively. These data indicate that RbC^N phosphorylation functions in a manner that is functionally compatible with the mechanisms induced by phosphorylation of Rb^{IDL} and Rb^{PL}, lending insight into the way that these three separate structural mechanisms contribute to the inhibition of Rb-$E2F^{TD}$ binding.

Phosphorylation mechanisms regulate E2Fs differently

The E2F family of transcription factors consists of members that both activate transcription (E2F1–3) and repress transcription (E2F4–8). During G_0 and early G_1, Rb negatively regulates transcription by binding and repressing activating E2F1–3, whereas the Rb paralogs p107 and p130 associate with repressive E2F4 and E2F5 [32]. E2F1–5 display a large degree of sequence and structural similarity, and crystal structures of $E2F1^{TD}$ and $E2F2^{TD}$ bound to Rb pocket reveal mostly similar binding modes. There are some notable, albeit subtle, differences in binding. For example, $E2F2^{TD}$ makes additional salt bridge and hydrogen bond contacts through D410 and D411, which are not observed in the structure of Rb-$E2F1^{TD}$ [10,11]. These differences in binding contacts suggest that E2Fs may be differentially affected by the distinct phosphorylation-induced mechanisms for E2F release.

We compared binding of $E2F1^{TD}$, $E2F2^{TD}$, and $E2F3^{TD}$ to Rb constructs designed to promote the specific phosphorylation-induced structural mechanisms we have identified for inhibiting $E2F^{TD}$ binding. These ITC data are summarized in Table 2 and shown in Supplementary Fig. S4. Previously, we found that phosphorylation of Rb^{IDL} (T356/T373) inhibits $E2F1^{TD}$ binding to Rb pocket 45-fold [25]. When we perform this experiment using the other activating E2Fs, we find that $E2F3^{TD}$ binding is inhibited 25-fold, while $E2F2^{TD}$ binding is inhibited only 2-fold. Phosphorylation of Rb^{PL} (S608/S612) and RbC^N (S788/S795) raise the K_d for Rb-$E2F3^{TD}$ binding 9-fold and 10-fold, respectively. These effects are similar to what is observed for $E2F1^{TD}$ [25]; however, we also observe that either of these mechanisms alone produces only a relatively smaller 3- to 4-fold inhibition of $E2F2^{TD}$ binding. When we test the effect of phosphorylating Rb^{IDL} and RbC^N together, we observe a larger 22-fold reduction in the binding affinity of $E2F2^{TD}$, suggesting that these mechanisms have a cooperative effect in dissociating $E2F2^{TD}$ from Rb.

These results support several conclusions regarding how phosphorylation modulates differently the interaction between Rb and the activating E2Fs. First, the Rb-$E2F2^{TD}$ interaction is distinct from $E2F1^{TD}$ and $E2F3^{TD}$ in that individual phosphorylation events produce little effect. Second, $E2F1^{TD}$ and $E2F2^{TD}$ have considerably higher affinity for unphosphorylated Rb than $E2F3^{TD}$. Therefore, like for $E2F2^{TD}$, multiple phosphorylation events on Rb are required for changing the $E2F1^{TD}$ affinity to the micromolar range. With its weaker initial affinity, $E2F3^{TD}$ may only require any one phosphorylation event for micromolar affinity. Finally, we note that, in the context of full-length phosphorylated Rb, it was observed that deletion of RbC has no effect on the inhibition of $E2F1^{TD}$ binding [25]. We suggest that the inhibitory effect of RbC^N phosphorylation observed here may not be additive with both Rb^{IDL} and Rb^{PL} phosphorylation together. Another possible explanation is that the association between RbC and the pocket induced by T821/T826 phosphorylation negatively influences the ability of phosphorylated RbC^N to bind the pocket and inhibit $E2F^{TD}$. Further exploration of the interdependence of phosphorylation events and their corresponding structural changes is needed to address these possibilities.

Table 2. ITC measurements of $E2F2^{TD}$ and $E2F3^{TD}$ binding to unphosphorylated and phosphorylated Rb constructs with different mechanisms of $E2F^{TD}$ binding inhibition.

Rb construct	Available CDK sites	Rb-$E2F2^{TD}$ K_d (μM)	PhosRb-$E2F2^{TD}$ K_d (μM)	Rb-$E2F3^{TD}$ K_d (μM)	PhosRb-$E2F3^{TD}$ K_d (μM)
$380\text{-}787^{S780A}$	S608/S612	0.04 ± 0.01	0.13 ± 0.01	1.2 ± 0.1	10.8 ± 0.4
$380\text{-}800^{\Delta PL/S780A}$	S788/S795	0.04 ± 0.03	0.15 ± 0.09	0.4 ± 0.1	3.8 ± 0.2
$53\text{-}787^{\Delta NL/\Delta PL/S780A}$	T356/T373	0.09 ± 0.04	0.2 ± 0.1	1.0 ± 0.3	24 ± 17
$53\text{-}800^{\Delta NL/\Delta PL/S780A}$	T356/T373/S788/S795	0.03 ± 0.01	0.68 ± 0.07	—	—

ITC data are shown in Supplementary Fig. S2.

Discussion

Rb inactivation by multisite phosphorylation is required for cell cycle advancement into S-phase and is commonly found in tumors. The studies presented here reveal a novel phosphorylation-induced mechanism that utilizes RbC and contributes to inhibition of the Rb-E2F growth-repressive complex. Our data demonstrate that S788/S795 phosphorylation plays a dual role in disrupting both the RbC-E2F1-DP1^{CM} and Rb pocket-E2F^{TD} interfaces. Our NMR data support a model in which phosphorylation of these sites stabilizes binding of RbC^{N} to the pocket domain. The interdomain association is likely mediated by other amino acids surrounding the phosphate moieties and takes place at a site that overlaps with the E2F^{TD} binding site.

Our analysis indicates that RbC^{N} phosphorylation enhances repression of E2F^{TD} binding induced by either Rb^{PL} or Rb^{IDL} phosphorylation, indicating that these pairwise mechanisms are functionally compatible. The additive inhibition of these phosphorylation events is consistent with their known and proposed structural effects. The binding site for phosphorylated RbC^{N} in the pocket domain near K652/R656 suggests that phosphorylated RbC^{N}, like Rb^{IDL} phosphorylation, disrupts interactions between the pocket and the N-terminal section of E2F^{TD} (Fig. 3) [26]. Alternatively, Rb^{PL} phosphorylation targets a separate Rb-E2F^{TD} interface near the C-terminus of E2F^{TD} [26]. We propose that the additive effect of RbC^{N} and Rb^{PL} phosphorylation in inhibiting Rb-E2F^{TD} binding occurs because these two mechanisms each targets a distinct, stabilizing subsection of the overall Rb-E2F^{TD} interface. We find that S807/S811 phosphorylation does not contribute to inhibition of the Rb-E2F^{TD} interaction either alone or in the presence of S788/S795. Although it remains a formal possibility that these residues contribute in some unique way to the regulation of Rb-E2F, other roles for these phosphoacceptor sites have been suggested, including modulating interactions with other proteins and serving as priming sites for subsequent phosphorylation events [24,29,33].

The quantitative binding studies presented here are consistent with cell-based studies, which indicate that S788/S795 phosphorylation plays a role in the dissociation of Rb-E2F complexes and E2F transactivation that is additive with other sites. Transcriptional assays using alanine substitutions at S788 and S795 show that these mutations alone are not sufficient to suppress E2F activation in the presence of kinase [30]. However, these mutations do greatly enhance the effects of additional phosphoacceptor mutations in suppressing E2F activity in the presence of kinase. A similar study confirms that S795 phosphorylation alone is insufficient to induce E2F activity [34]. In cells, S795 phosphorylation is most likely the target of CDK4, and not CDK2 [21,35,36]. More recent studies have shown that S795 phosphorylation and E2F activation also occur in response to p38 activation [37,38].

We tested for the first time here the specific effects of each phosphorylation mechanism on different activating E2F transactivation domains. We found that, while discrete phosphorylation at T356/T373, S608/S612, or S788/S795 reduces the affinity of Rb for E2F1^{TD} or E2F3^{TD} nearly 10-fold in each case, the effect of phosphorylating one pair of sites on E2F2^{TD} binding is modest. Phosphorylation of both Rb^{IDL} and RbC^{N} sites together dramatically reduces E2F2^{TD}. While we do not understand the details explaining this synergy and its specificity for E2F2^{TD}, we note that E2F2^{TD} makes specific additional contacts relative to E2F1^{TD} in the region of the pocket domain most affected by the structural changes induced by RbC^{N} and Rb^{IDL} phosphorylation.

The observation that E2F1^{TD} and E2F2^{TD} are less responsive to activation by specific phosphorylation events than E2F3^{TD} is noteworthy considering that activating E2Fs have distinct cellular functions, regulate only partially overlapping sets of genes, and show differences in how they regulate expression in conjunction with other transcription factors and post-translational modifications [32,39,40]. We suggest that such differential effects of phosphorylation provide a possible mechanism for tuning different E2F family member activities separately. Further identification of specific Rb phosphorylation events in different cellular contexts remains an important goal for understanding when and how these mechanisms contribute to Rb regulation of E2F activity.

Materials and Methods

Protein expression, purification, and phosphorylation

Rb and E2F protein constructs were expressed in *Escherichia coli* as fusion proteins with glutathione *S*-transferase (GST). Cells were induced overnight at room temperature with the exception of RbC$^{787\text{-}816}$, which was induced for 2.5 h at 37 °C. Cells were re-suspended in a lysate buffer containing 100 mM NaCl, 25 mM Tris–HCl (pH 8.0), 1 mM PMSF, and 1 mM dithiothreitol; passed twice through a cell homogenizer; and centrifuged at 27,000*g* for 30 min. The supernatant fraction of the lysate was loaded to GS4B affinity resin and eluted with 10 mM glutathione. Eluate was further purified using anion-exchange chromatography. The GST tag was cleaved overnight at 4 °C with 1% (percentage mass of substrate in the reaction) GST-tagged tobacco etch virus, and the cleaved protein was passed back over GS4B resin to remove GST. E2F1-DP1^{CM} was prepared and purified as described previously [14].

Purified Rb protein was phosphorylated by concentrating to 4 mg/mL and incubating in a reaction containing 5% CDK2-CyclinA, 10 mM ATP, 10 mM $MgCl_2$, 100 mM NaCl,

25 mM Tris–HCl (pH 8.0), and 1 mM dithiothreitol at 4 °C overnight. Quantitative phosphorylation of $RbC^{787-816}$ could be achieved but required using 5% CDK2-CyclinA and 2% CDK6-CyclinK. Proteins were analyzed for phosphate incorporation using electrospray ionization mass spectrometry as previously described [25]. A sample mass spectrometry experiment demonstrating quantitative phosphorylation is shown in Supplementary Fig. S2.

NMR spectroscopy

All samples were prepared in a buffer containing 50 mM $NaPO_4$, 5 mM dithiothreitol, and 10% D_2O (pH 6.1). $^1H–^{15}N$ HSQC spectra were recorded at 25 °C on a Varian INOVA 600-MHz spectrometer equipped with a 5-mm HCN cryoprobe. HSQC assignments for ^{15}N-labeled phosphorylated $RbC^{787-816}$ were obtained using $^1H–^{15}N$ side-chain correlations observed in a three-dimensional $^1N–^{15}N$ total correlated spectroscopy spectrum (120 ms mixing time) and a three-dimensional $^1N–^{15}N$ nuclear Overhauser enhancement spectroscopy spectrum (360 ms mixing time) [41,42]. All NMR spectra were processed with NMRPipe and analyzed with NMRViewJ [43,44].

Isothermal titration calorimetry

ITC experiments were conducted with a MicroCal VP-ITC calorimeter. Proteins were dialyzed overnight in a buffer containing 100 mM NaCl, 25 mM Tris–HCl (pH 8.0), and 1 mM dithiothreitol. The data were fit to one-site binding using the Origin software package. Reported error values reflect the standard deviation of 2–4 separate binding experiments. In all cases, the stoichiometry parameter was determined to be around $n \sim 1$.

Supplementary data to this article can be found online at http://dx.doi.org/10.1016/j.jmb.2013.09.031.

Received 28 August 2013;
Accepted 20 September 2013
Available online 5 October 2013

Keywords:
cell cycle regulation;
multisite phosphorylation;
cyclin-dependent kinases;
Rb protein;
protein–protein interactions

Abbreviations used:
CDK, cyclin-dependent kinase; ITC, isothermal titration calorimetry; HSQC, heteronuclear single quantum coherence; GST, glutathione S-transferase.

References

[1] Burkhart DL, Sage J. Cellular mechanisms of tumour suppression by the retinoblastoma gene. Nat Rev Cancer 2008;8:671–82.
[2] Dick FA, Rubin SM. Molecular mechanisms underlying RB protein function. Nat Rev Mol Cell Biol 2013;14:297–306.
[3] Buchkovich K, Duffy LA, Harlow E. The retinoblastoma protein is phosphorylated during specific phases of the cell cycle. Cell 1989;58:1097–105.
[4] Chen PL, Scully P, Shew JY, Wang JY, Lee WH. Phosphorylation of the retinoblastoma gene product is modulated during the cell cycle and cellular differentiation. Cell 1989;58:1193–8.
[5] DeCaprio JA, Ludlow JW, Lynch D, Furukawa Y, Griffin J, Piwnica-Worms H, et al. The product of the retinoblastoma susceptibility gene has properties of a cell cycle regulatory element. Cell 1989;58:1085–95.
[6] Mihara K, Cao XR, Yen A, Chandler S, Driscoll B, Murphree AL, et al. Cell cycle-dependent regulation of phosphorylation of the human retinoblastoma gene product. Science 1989;246:1300–3.
[7] Bagchi S, Weinmann R, Raychaudhuri P. The retinoblastoma protein copurifies with E2F-I, an E1A-regulated inhibitor of the transcription factor E2F. Cell 1991;65:1063–72.
[8] Bandara LR, La Thangue NB. Adenovirus E1a prevents the retinoblastoma gene product from complexing with a cellular transcription factor. Nature 1991;351:494–7.
[9] Hagemeier C, Cook A, Kouzarides T. The retinoblastoma protein binds E2F residues required for activation *in vivo* and TBP binding *in vitro*. Nucleic Acids Res 1993;21:4998–5004.
[10] Lee C, Chang JH, Lee HS, Cho Y. Structural basis for the recognition of the E2F transactivation domain by the retinoblastoma tumor suppressor. Genes Dev 2002;16:3199–212.
[11] Xiao B, Spencer J, Clements A, Ali-Khan N, Mittnacht S, Broceno C, et al. Crystal structure of the retinoblastoma tumor suppressor protein bound to E2F and the molecular basis of its regulation. Proc Natl Acad Sci USA 2003;100:2363–8.
[12] Cecchini MJ, Dick FA. The biochemical basis of CDK phosphorylation-independent regulation of E2F1 by the retinoblastoma protein. Biochem J 2011;434:297–308.
[13] Dick FA, Dyson N. pRB contains an E2F1-specific binding domain that allows E2F1-induced apoptosis to be regulated separately from other E2F activities. Mol Cell 2003;12:639–49.
[14] Rubin SM, Gall AL, Zheng N, Pavletich NP. Structure of the Rb C-terminal domain bound to E2F1-DP1: a mechanism for phosphorylation-induced E2F release. Cell 2005;123:1093–106.
[15] Helin K, Lees JA, Vidal M, Dyson N, Harlow E, Fattaey A. A cDNA encoding a pRB-binding protein with properties of the transcription factor E2F. Cell 1992;70:337–50.
[16] Kaelin Jr WG, Krek W, Sellers WR, DeCaprio JA, Ajchenbaum F, Fuchs CS, et al. Expression cloning of a cDNA encoding a retinoblastoma-binding protein with E2F-like properties. Cell 1992;70:351–64.
[17] Qin XQ, Chittenden T, Livingston DM, Kaelin WG. Identification of a growth suppression domain within the retinoblastoma gene product. Genes Dev 1992;6:953–64.
[18] Lees JA, Buchkovich KJ, Marshak DR, Anderson CW, Harlow E. The retinoblastoma protein is phosphorylated on multiple sites by human cdc2. EMBO J 1991;10:4279–90.
[19] Lin BT, Gruenwald S, Morla AO, Lee WH, Wang JY. Retinoblastoma cancer suppressor gene product is a substrate of the cell cycle regulator cdc2 kinase. EMBO J 1991;10:857–64.
[20] Mittnacht S, Lees JA, Desai D, Harlow E, Morgan DO, Weinberg RA. Distinct sub-populations of the retinoblastoma protein show a distinct pattern of phosphorylation. EMBO J 1994;13:118–27.

[21] Zarkowska T, Mittnacht S. Differential phosphorylation of the retinoblastoma protein by G1/S cyclin-dependent kinases. J Biol Chem 1997;272:12738–46.
[22] Chellappan SP, Hiebert S, Mudryj M, Horowitz JM, Nevins JR. The E2F transcription factor is a cellular target for the RB protein. Cell 1991;65:1053–61.
[23] Hamel PA, Gill RM, Phillips RA, Gallie BL. Regions controlling hyperphosphorylation and conformation of the retinoblastoma gene product are independent of domains required for transcriptional repression. Oncogene 1992;7:693–701.
[24] Rubin SM. Deciphering the retinoblastoma protein phosphorylation code. Trends Biochem Sci 2013;38:12–9.
[25] Burke JR, Deshong AJ, Pelton JG, Rubin SM. Phosphorylation-induced conformational changes in the retinoblastoma protein inhibit E2F transactivation domain binding. J Biol Chem 2010;285:16286–93.
[26] Burke JR, Hura GL, Rubin SM. Structures of inactive retinoblastoma protein reveal multiple mechanisms for cell cycle control. Genes Dev 2012;26:1156–66.
[27] Lamber EP, Beuron F, Morris EP, Svergun DI, Mittnacht S. Structural insights into the mechanism of phosphoregulation of the retinoblastoma protein. PLoS One 2013;8:e58463.
[28] Harbour JW, Luo RX, Dei Santi A, Postigo AA, Dean DC. Cdk phosphorylation triggers sequential intramolecular interactions that progressively block Rb functions as cells move through G1. Cell 1999;98:859–69.
[29] Knudsen ES, Wang JY. Differential regulation of retinoblastoma protein function by specific Cdk phosphorylation sites. J Biol Chem 1996;271:8313–20.
[30] Brown VD, Phillips RA, Gallie BL. Cumulative effect of phosphorylation of pRB on regulation of E2F activity. Mol Cell Biol 1999;19:3246–56.
[31] Knudsen ES, Wang JY. Dual mechanisms for the inhibition of E2F binding to RB by cyclin-dependent kinase-mediated RB phosphorylation. Mol Cell Biol 1997;17:5771–83.
[32] Trimarchi JM, Lees JA. Sibling rivalry in the E2F family. Nat Rev Mol Cell Biol 2002;3:11–20.
[33] Ren S, Rollins BJ. Cyclin C/Cdk3 promotes Rb-dependent G0 exit. Cell 2004;117:239–51.
[34] Gorges LL, Lents NH, Baldassare JJ. The extreme COOH terminus of the retinoblastoma tumor suppressor protein pRb is required for phosphorylation on Thr-373 and activation of E2F. Am J Physiol Cell Physiol 2008;295:C1151–60.
[35] Connell-Crowley L, Harper JW, Goodrich DW. Cyclin D1/Cdk4 regulates retinoblastoma protein-mediated cell cycle arrest by site-specific phosphorylation. Mol Biol Cell 1997;8:287–301.
[36] Grafstrom RH, Pan W, Hoess RH. Defining the substrate specificity of cdk4 kinase-cyclin D1 complex. Carcinogenesis 1999;20:193–8.
[37] Garnovskaya MN, Mukhin YV, Vlasova TM, Grewal JS, Ullian ME, Tholanikunnel BG, et al. Mitogen-induced rapid phosphorylation of serine 795 of the retinoblastoma gene product in vascular smooth muscle cells involves ERK activation. J Biol Chem 2004;279:24899–905.
[38] Wang S, Nath N, Minden A, Chellappan S. Regulation of Rb and E2F by signal transduction cascades: divergent effects of JNK1 and p38 kinases. EMBO J 1999;18:1559–70.
[39] Giangrande PH, Hallstrom TC, Tunyaplin C, Calame K, Nevins JR. Identification of E-box factor TFE3 as a functional partner for the E2F3 transcription factor. Mol Cell Biol 2003;23:3707–20.
[40] Schlisio S, Halperin T, Vidal M, Nevins JR. Interaction of YY1 with E2Fs, mediated by RYBP, provides a mechanism for specificity of E2F function. EMBO J 2002;21:5775–86.
[41] Mori S, Abeygunawardana C, Johnson MO, van Zijl PC. Improved sensitivity of HSQC spectra of exchanging protons at short interscan delays using a new fast HSQC (FHSQC) detection scheme that avoids water saturation. J Magn Reson Ser B 1995;108:94–8.
[42] Norwood TJ, Boyd J, Heritage JE, Soffe N, Campbell ID. Comparison of techniques for ^{1}H-detected heteronuclear ^{1}H–^{15}N spectroscopy. J Magn Reson 1990;87:488–501.
[43] Delaglio F, Grzesiek S, Vuister GW, Zhu G, Pfeifer J, Bax A. NMRPipe: a multidimensional spectral processing system based on UNIX pipes. J Biomol NMR 1995;6:277–93.
[44] Johnson BA, Blevins RA. NMR View: a computer program for the visualization and analysis of NMR data. J Biomol NMR 1994;4:603–14.